Nucleic Acids Research, 2005, Vol. 33, No. 9 ***2993–3001***
doi:10.1093/nar/gki610

Human XPC-hHR23B interacts with XPA-RPA in the recognition of triplex-directed psoralen DNA interstrand crosslinks

Brian S. Thoma, Mitsuo Wakasugi[1], Jesper Christensen[2], Madhava C. Reddy and Karen M. Vasquez*

Department of Carcinogenesis, The University of Texas M. D. Anderson Cancer Center, Science Park—Research Division, Smithville, TX 78957, USA, [1]Faculty of Pharmaceutical Sciences, Kanazawa University, Takara-machi, Kanazawa 920-0934, Japan and [2]Biotech Research and Innovation Centre, Fruebjergvej 3, 2100 Copenhagen, Denmark

Received February 4, 2005; Revised and Accepted May 3, 2005

ABSTRACT

DNA interstrand crosslinks (ICLs) represent a severe form of damage that blocks DNA metabolic processes and can lead to cell death or carcinogenesis. The repair of DNA ICLs in mammals is not well characterized. We have reported previously that a key protein complex of nucleotide excision repair (NER), XPA-RPA, recognizes DNA ICLs. We now report the use of triplex technology to direct a site-specific psoralen ICL to a target DNA substrate to determine whether the human global genome NER damage recognition complex, XPC-hHR23B, recognizes this lesion. Our results demonstrate that XPC-hHR23B recognizes psoralen ICLs, which have a structure fundamentally different from other lesions that XPC-hHR23B is known to bind, with high affinity and specificity. XPC-hHR23B and XPA-RPA protein complexes were also observed to bind psoralen ICLs simultaneously, demonstrating not only that psoralen ICLs are recognized by XPC-hHR23B alone, but also that XPA-RPA may interact cooperatively with XPC-hHR23B on damaged DNA, forming a multimeric complex. Since XPC-hHR23B and XPA-RPA participate in the recognition and verification of DNA damage, these results support the hypothesis that interplay between components of the global genome repair sub-pathway of NER is critical for the recognition of psoralen DNA ICLs in the mammalian genome.

INTRODUCTION

Most bulky DNA lesions are processed by the nucleotide excision repair (NER) pathway, which is composed of two sub-pathways: transcription coupled repair (TCR) and global genome repair (GGR). Lesions that inhibit DNA transcription are believed to be the principle targets of the TCR pathway. Experimental evidence has shown that RNA Pol II progression along transcribed DNA is sensitive to the presence of DNA damage, leading to the hypothesis that interruption of RNA Pol II processivity could serve as the initiating signal for TCR (1,2). Other constituents of this pathway (such as Cockayne Syndrome Group A and B proteins) may also assist in the identification of DNA damage (3–7). The GGR sub-pathway of NER is believed to be responsible for detecting and repairing bulky DNA lesions over the entire genome with the exception of those genes undergoing active transcription. Although NER has been extensively studied, it is still debatable exactly which proteins are responsible for recognition of specific lesions in GGR and TCR since a number of different proteins, including *Xeroderma pigmentosum* protein Group C-human homolog of RAD23B (XPC-hHR23B), replication protein A (RPA) and *X.pigmentosum* protein Group A (XPA), each bind to many DNA lesions that are substrates for NER [reviewed in (8)].

Among the many different kinds of DNA damage, DNA interstrand crosslinks (ICLs) are among the most detrimental to DNA metabolism and are lethal in repair deficient prokaryotic and eukaryotic cells (9). Both NER and homologous recombination (HR) mechanisms are involved in repairing DNA ICLs in bacteria and yeast (10–12), but the mechanisms of repair of crosslinked DNA in mammalian cells are not well characterized. A number of crosslinking agents, including the psoralen family of intercalating, photoactivatable DNA damaging agents, are available for the study of the repair of DNA ICLs. Following irradiation with ultraviolet-A (UVA) light, psoralen molecules form DNA crosslinks between thymines on opposing strands of duplex DNA. Psoralen plus UVA

*To whom correspondence should be addressed. Tel: +512 237 9324; Fax: +512 237 2475; Email: kvasquez@sprd1.mdacc.tmc.edu

(PUVA) therapy has been effectively utilized as a treatment for psoriasis and cutaneous T-cell lymphoma, primarily due to its ability to induce DNA ICLs that result in the inhibition of DNA metabolism, induction of DNA mutations and cellular toxicity (9,13). The preferred psoralen crosslinking site is a 5′-TpA, yet psoralens demonstrate minimal sequence specificity when intercalating into the DNA. DNA triplex technology has been successfully employed as a means to target psoralen in a site-specific manner to generate a single, unique DNA cross-link (14–16). This specificity is accomplished by conjugating a psoralen molecule to a triplex-forming oligonucleotide (TFO) designed to bind with high affinity and specificity, via Hoogsteen or reverse-Hoogsteen hydrogen bonds, to a purine-rich triplex recognition sequence on a target DNA duplex [reviewed in (17)]. Targeting DNA damage via triplex formation has been used successfully *in vitro* and *in vivo* to induce site-specific DNA mutations, DNA recombination and to study DNA–protein interactions at a specific site (17–22). We have previously demonstrated that DNA damage recognition proteins, including the NER proteins RPA and XPA, will bind to triplex DNA substrates containing a single psoralen ICL (22). Although both RPA and XPA likely play roles in detecting DNA lesions (including DNA ICLs), there is very compelling evidence suggesting that XPC-hHR23B is the principle damage recognition factor in GGR [reviewed in (8) and references therein]. Because of the critical role that XPC-hHR23B appears to play in identifying DNA damage, we were interested in whether XPC-hHR23B would recognize a complex lesion such as a TFO-directed psoralen-DNA ICL.

In this work the capacity of XPC-hHR23B, or XPC-hHR23B in combination with XPA-RPA, to recognize a unique TFO-directed psoralen-interstrand crosslink (Tdp-ICL) on a DNA substrate was investigated. Previously, others have shown that XPC-hHR23B recognizes substrates containing *cis*-platin-DNA intrastrand-crosslinks (23–26) and psoralen-monoadducted DNA (27). Our results provide the first demonstration that the human recombinant XPC-hHR23B protein complex interacts with a Tdp-ICL with high affinity and specificity. XPC-hHR23B was also observed to bind to complexes formed between psoralen damaged DNA and the XPA-RPA NER recognition complex. At low XPA-RPA concentrations, XPC-hHR23B and XPA-RPA compete for binding to the lesion, but at higher RPA concentrations XPC-hHR23B and XPA-RPA bound a damaged DNA substrate together to form a high molecular weight multimeric complex. Our observations implicate human XPC-hHR23B in the recognition of DNA ICLs and demonstrate a possible positive interaction between XPC-hHR23B and XPA-RPA in the recognition of these lesions. Thus, these data support a role for the GGR subpathway of NER in the recognition of Tdp-ICLs in the mammalian genome.

MATERIALS AND METHODS

Oligonucleotides

Synthetic duplex targets for TFO binding from the APRT and pSupFG1 triplex target sites were constructed as described previously (22). pTFO1 (19mer) binds to the corresponding 19 bp polypurine site in the APRT-derived duplex (37 bp) target and pTFOc is a 19 base scrambled oligonucleotide that does not bind the APRT target (16). pAG30 (30mer) forms a triplex DNA structure on a 30 bp polypurine site on the 57-bp pSupFG1-derived sequence and pSCR30 is a 30 base scrambled control oligonucleotide (22). TFOs were synthesized with a 5′-psoralen derivative, HMT, (2-[4′(hydroxymethyl)-4,5′,8-trimethylpsoralen]-hexyl-1-*O*-(2-cyanoethyl)-*N*,*N*-diisopropyl)-phosphoramidite) by the Midland Certified Reagent Company, Inc. (Midland, TX). Duplexes were 5′ end-labeled by the transfer of ^{32}P from [γ-^{32}P]dATP with T4 polynucleotide kinase and purified by 12% PAGE, electroeluted and concentrated via Centricon centrifugal filtration devices (Millipore, Bedford, MA). DNA concentration was determined by UV absorbance at 260 nm.

Tdp-ICL formation

Triplex substrates were generated by incubating radiolabeled duplex targets with psoralen-conjugated TFOs in a triplex binding buffer [10 mM Tris–HCl, pH 7.6, 10 mM $MgCl_2$ and 10% (v/v) glycerol] at 37°C for 16 h. Samples were then irradiated with 1.8 J/cm^2 of UVA light at 366 nm to induce psoralen ICLs. Efficiency of crosslinking at the targeted triplex-duplex junction was as high as 90%, as determined by the quantification of the crosslinked product by denaturing PAGE using a phosphorimager (Figure 1). All Tdp-ICL substrates were gel purified to remove free duplex DNA (unless stated otherwise) prior to use.

Human recombinant proteins

The XPC-hHR23B-maltose-binding protein fusion protein was expressed and purified in Sf9 or Hi-5 insect cells as described previously (28,29). Recombinant XPA-maltose-binding protein fusion protein was expressed in *Escherichia coli* PR745 and purified as described previously (30). For recombinant RPA, the three subunits were expressed by co-infection of Sf9 insect cells and purified by Ni^{2+}-chelate column chromatography as previously described (31).

DNA–protein binding assays

DNA–protein binding interactions were analyzed by electrophoretic mobility shift assays (EMSAs). Human recombinant proteins, at varying concentrations, were incubated in binding buffer [25 mM Tris–HCl, pH 7.6, 100 mM NaCl, 1 mM DTT, 5 mM EDTA, 100 μg/ml BSA, 0.01% NP-40 (v/v) and 10% glycerol (v/v)] in a 20 μl reaction volume for 10 min at room temperature (unless otherwise stated). Radiolabeled duplex or triplex substrates were then added and incubated at 30°C for 20 min. In the sequential addition experiments, the protein used at the static concentration was incubated with the Tdp-ICL substrate for 10 min, then increasing concentrations of the other protein were added. In the simultaneous experiments, proteins were incubated together for 10 min at room temperature in binding buffer, and then the Tdp-ICL substrate was added. The DNA–protein samples were then electrophoresed through a 6% (37.5:1 acrylamide/bis-acrylamide) native PAGE, containing 2.5% glycerol and buffered in 1× TGE (25 mM Tris–HCl, 192 mM glycine and 1 mM EDTA). Electophoresis was conducted at 4°C, 9 mA/cm for 3 h. Gels were dried and DNA–protein complexes were visualized by autoradiography and quantified using a phosphorimager.

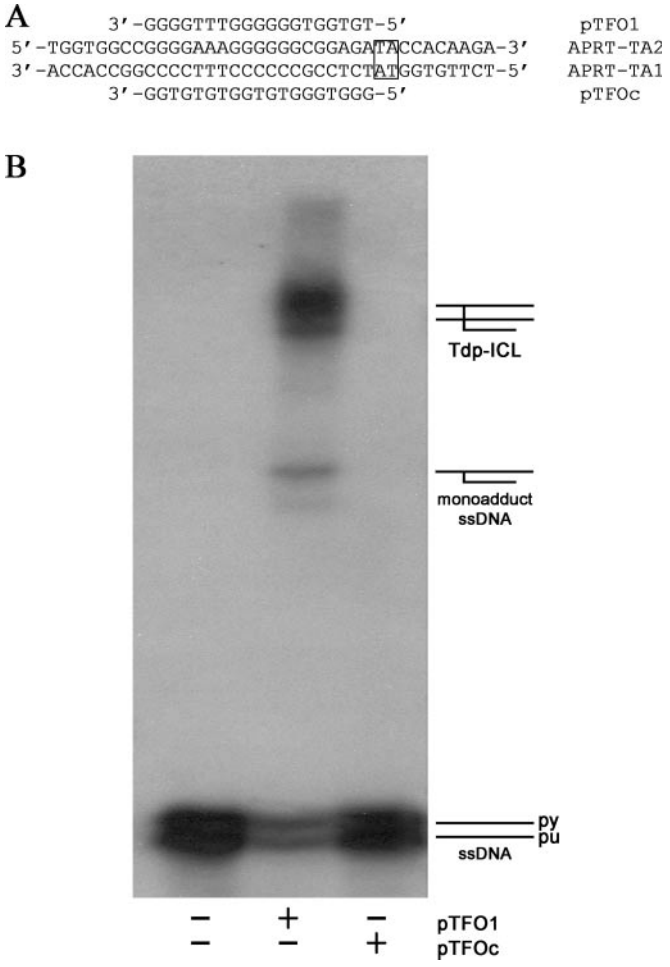

Figure 1. Electrophoretic analysis of photoadducts formed by pTFO1 on the APRT-TA synthetic DNA duplex. (**A**) Sequence of the APRT-TA (37 bp) synthetic duplex is shown with the 5′-TpA psoralen crosslinking site boxed. The psoralen-conjugated specific TFO, pTFO1, and the scrambled control, pTFOc, are shown. (**B**) TFOs were incubated with a ^{32}P-end-labeled APRT-TA DNA target duplex, then UVA-irradiated at 1.8 J/cm^2 to allow formation of a site-specific Tdp-ICL. Crosslinking efficiency was determined by denaturing 15% PAGE and quantified by phosphorimage analysis. Diagramatic representations of Tdp-ICLs, monoadducted single-strand DNA and denatured duplex are shown to the right of the figure. The label py stands for pyrimidine-rich strand (top strand in Figure 1A) and pu for purine-rich strand (bottom strand in Figure 1A).

Apparent half-maximal binding of the available substrate is defined as 'K_{app}'.

Kinetic assay

DNA–protein complexes were formed as described above, except that incubations were carried out for <10 s, 1, 2 or 4 min. The shortest time point was defined as the time required to add protein(s) to the DNA substrate immediately prior to loading the reaction on the native PAG at 4°C (actual incubation time of protein with DNA substrate was <10 s at 4°C).

Antibody super-shift assay

DNA–protein complexes were formed as described above. Next, monoclonal antibodies directed against RPA (anti-RPA$_{34}$; Lab Vision, Fremont, CA) or the maltose-binding protein tag on the human recombinant XPC-hHR23B (anti-MBP; New England Biolabs, Beverly, MA) were added to the DNA–protein complexes (1 μg/20 μl reaction) and incubated at 30°C for 10 min. Following incubation, the reactions were electrophoresed through a 4 or 5% (37.5:1 acrylamide/bis-acrylamide) native PAG in 1× TGE buffer at 4°C, 200 V for 4 h. Gels were dried and the separated complexes were visualized by autoradiography and quantified using a phosphorimager.

RESULTS

Formation of Tdp-ICLs

Figure 1A depicts the 37 bp APRT-TA target duplex for the 19 nt psoralen-conjugated oligonucleotides, pTFO1 (the specific TFO), and pTFOc (the control oligonucleotide that does not bind the APRT-TA sequence). Psoralen photomodification efficiency was determined by incubating the psoralen-modified TFOs with the radiolabeled target duplex, APRT-TA, to allow triplex formation, followed by UVA irradiation of the samples at 1.8 J/cm^2. The samples were then subjected to denaturing PAGE (Figure 1B) and the crosslinked population was quantified by phosphorimage analysis. Psoralen crosslinked product (Tdp-ICL) was formed with high efficiency (⩾85%), while the amount of crosslinked product formed with the control TFO, pTFOc represented less that 1% of the population, demonstrating that pTFO1 is capable of supporting a high level of site-specific DNA ICL formation.

Recognition of Tdp-ICL substrate by the human recombinant XPC-hHR23B protein complex

The XPC-hHR23B complex has been proposed to be the initial damage recognition factor in GGR, although XPA and RPA have also been implicated [recently reviewed in (8)]. Since we have shown previously that the XPA and RPA NER proteins bind to Tdp-ICLs (22), we wanted to determine whether XPC-hHR23B also interacts with these lesions. To address this question, Tdp-ICLs were formed on ^{32}P-end-labeled duplex DNA substrates of different sizes (37 and 57 bp) and incubated with increasing concentrations of human recombinant XPC-hHR23B (0.13, 1.3 and 6.5 nM). XPC-hHR23B bound both Tdp-ICL substrates, except at the lowest protein concentration (data not shown). To determine whether the binding of the Tdp-ICL by XPC-hHR23B was dependent on the triplex structure induced by the TFO, a similar binding experiment was performed on a TFO-directed psoralen ICL (following removal of the third strand TFO). The results indicated that XPC-hHR23B does bind the psoralen ICL in the absence of triplex formation, but with slightly lower affinity (data not shown).

XPC-hHR23B binds with high specificity to a Tdp-ICL in a concentration dependent manner

It has been reported that XPC-hHR23B interacts with both damaged and undamaged DNA (24,25,32,33). In order to ascertain specificity of XPC-hHR23B binding to ICL-damaged DNA, XPC-hHR23B's affinity for the Tdp-ICL substrate was compared to its binding to an undamaged DNA substrate. The Tdp-ICL substrate was incubated with increasing concentrations of XPC-hHR23B (from 0 to 13 nM) and recognition of the Tdp-ICL was detected at concentrations as

low as 1.3 nM (Figure 2, lane 9), with half-maximal binding (K_{app}) at a concentration of 6.5 nM (Figure 2, lane 11). A separate binding titration (to saturation) experiment was also conducted by incubating increasing concentrations of XPC-hHR23B with the Tdp-ICL substrate until essentially 100% of the substrate was bound (at 65 nM XPC-hHR23B; data not shown). Throughout the range of protein concentrations tested, the amount of unbound Tdp-ICL substrate decreased with increasing concentrations of XPC-hHR23B, while the amount of unbound duplex DNA did not change. Recombinant XPC-hHR23B (at concentrations $\geqslant$6.5 nM) was observed to bind the undamaged duplex DNA substrate, however phosphorimage analysis revealed that $\leqslant$1% of the available substrate was bound at even the highest concentration (13 nM) of XPC-hHR23B (data not shown). Separate experiments revealed that the binding profile of XPC-hHR23B to duplex DNA plus a control psoralen-modified oligonucleotide (that does not bind the duplex target site) was indistinguishable from that seen for protein incubated with duplex DNA only, as expected (data not shown). These results confirm that XPC-hHR23B specifically binds the Tdp-ICL substrate, and supports previous observations by others that XPC-hHR23B binds undamaged duplex DNA, but at a lower level than its binding to a damaged DNA substrate (24,25,32,33).

Interactions of Human Recombinant XPC-hHR23B and XPA-RPA on Tdp-ICLs

We have previously demonstrated that both RPA and XPA can bind to the Tdp-ICL substrate used in the experiments herein and that XPA appeared to modify RPA's interaction on these lesions (22). Unique interactions among XPC-hHR23B, TFIIH and XPA on different types of DNA damage have also been demonstrated (34–38). Thus, we were interested in the potential interactions of RPA and/or XPA with XPC-hHR23B on a Tdp-ICL substrate. In addition, we wanted to investigate whether the order in which the proteins were added to the reaction would influence any interactions of the proteins on these lesions. In these experiments the concentration of XPC-hHR23B was held constant at 6.5 nM (K_{app} concentration) while increasing concentrations of RPA (0.45–23.0 nM) and/or XPA (1.6–160 nM) were added to the reaction. In other experiments, the amount of XPC-hHR23B was varied (from 0.26 to 13.0 nM) while RPA and/or XPA were held constant at concentrations of 4.5 and 160 nM, respectively. As reported previously (22), XPA alone did not appear to shift the Tdp-ICL substrate in gel-shift assays (Figure 6, lane 2). Furthermore, recognition of the Tdp-ICL substrate by XPC-hHR23B did not appear to be affected by XPA at any of the concentrations tested, regardless of when it was introduced into the reaction with XPC-hHR23B and DNA substrate (data not shown). Interestingly, RPA and XPC-hHR23B did appear to influence each other when both proteins were present in the reaction (Figure 3A and B), with a biphasic dependence on RPA concentrations. At low concentrations of RPA and XPC-hHR23B, they each form simple complexes with the

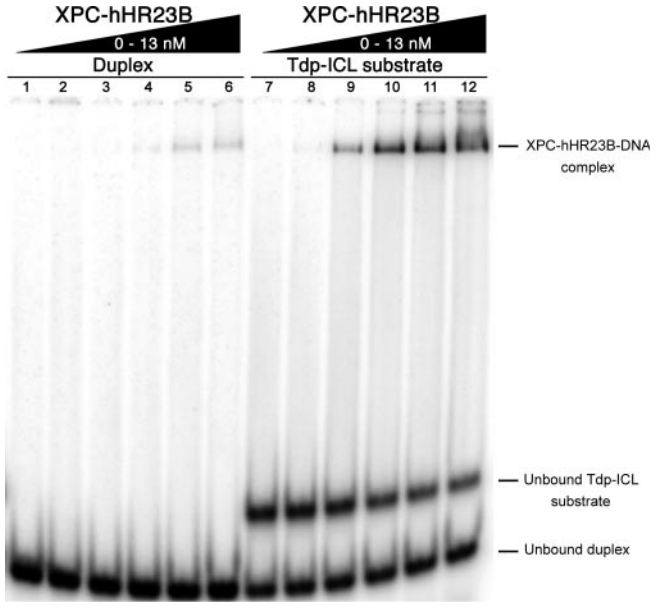

Figure 2. Human recombinant XPC-hHR23B recognizes Tdp-ICLs with high specificity and affinity. The psoralen-conjugated specific TFO, pTFO1, was UVA-crosslinked to a ^{32}P-end-labeled 37 bp APRT-TA DNA target duplex to form a site-specific Tdp-ICL. Varying concentrations of human recombinant XPC-hHR23B (at concentrations of 0, 0.13, 1.3, 3.3, 6.5 and 13.0 nM) were incubated with ^{32}P-end-labeled APRT-TA duplex (10 nM, lanes 1–6) or Tdp-ICL (10 nM, lanes 7–12) for 20 min at 30°C. DNA–protein complexes were electrophoretically separated on a 6% native PAG in 1× TGE buffer for 3 h at 9 mA/cm at 4°C. The gel was dried and the bands were visualized by autoradiography and quantified via phosphorimaging to determine the apparent dissociation constant (K_{app}).

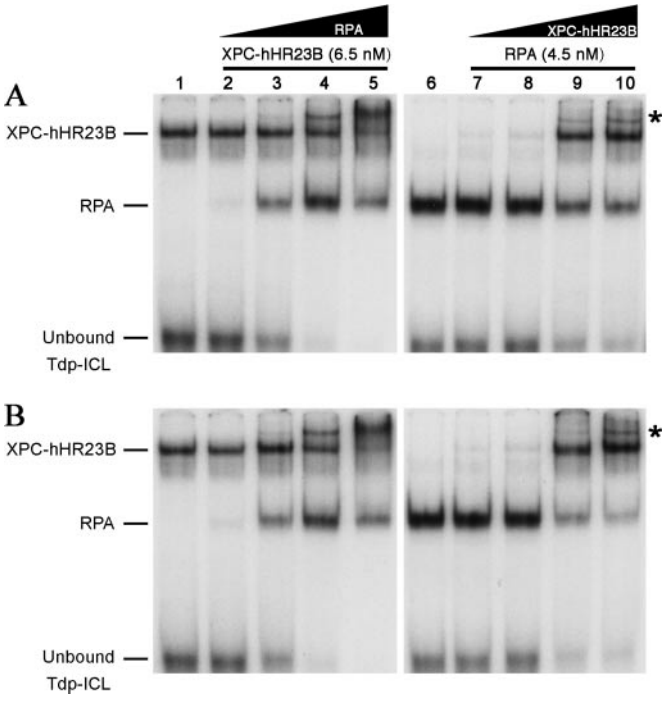

Figure 3. XPC-hHR23B and RPA interact to recognize a Tdp-ICL substrate to form a higher-order protein–DNA complex. Proteins were tested by both (**A**) sequential and (**B**) simultaneous addition to the Tdp-ICL. For these experiments XPC-hHR23B (Lanes 1–5) or RPA (lanes 6–10) were held steady at K_{app} concentration while the concentration of the other protein was varied. All DNA–protein reactions were incubated and separated by EMSA as described in the experimental procedures. Lane 1: XPC-hHR23B (6.5 nM) only. Lanes 2–5: XPC-hHR23B (6.5 nM) and RPA at 0.45, 4.5, 9.0 or 23.0 nM respectively. Lane 6: RPA (4.5 nM) only. Lanes 7–10: RPA (4.5 nM) and XPC-hHR23B at 0.26, 1.3, 6.5 or 13.0 nM, respectively. (*): indicates position of the higher order protein complex.

damaged DNA, and compete with one another for binding to DNA. At higher RPA concentrations (≥9 nM), higher order complexes are formed, when either XPC-hHR23B or RPA is added sequentially, or when they are added simultaneously. For example, a unique higher-order complex was detected with a slower mobility than that of the XPC-hHR23B-DNA complex [indicated by an asterisk, Figure 3A and B, compare lanes 3–5] in the presence of both XPC-hHR23B and RPA. This higher-order complex was initially observed when the concentration of XPC-hHR23B was held constant (6.5 nM) and RPA was added at a concentration of 11.3 nM (*, Figure 3A and B, lane 4). At protein concentrations of 6.5 and 23.0 nM for XPC-hHR23B and RPA, respectively, the higher-order complex (*, Figure 3A and B, lane 5) was calculated to represent nearly 50% of the bound substrate. A higher-order complex was also seen when RPA was held steady at 4.5 nM and XPC-hHR23B was present at 6.5 and 11.3 nM, but under these conditions it represented only a minor amount of the total shifted substrate (*, Figure 3A and B, lanes 9 and 10). These results were observed regardless of whether the proteins were added to the reaction sequentially (Figure 3A) or simultaneously (Figure 3B). When the experiments described above were performed with XPC-hHR23B and the XPA-RPA complex (rather than RPA alone), the results were indistinguishable from those presented in Figure 3.

Since the observations made in Figure 3 were based on changes in the protein concentration relative to each component's K_{app} concentration, the binding of these proteins to the Tdp-ICL substrate was also tested at equimolar concentrations. Proteins were added (in 10-fold increments) at concentrations ranging from 0.01 to 10 nM and allowed to incubate with the damaged DNA substrate. Similar to the results shown in Figure 3, the higher-order complex was only observed in the presence of high concentrations of RPA (10 nM) (data not shown).

Kinetic analysis of XPC-hHR23B and XPA-RPA recognition of a Tdp-ICL substrate

In order to determine the kinetic properties of XPC-hHR23B with XPA and RPA on Tdp-ICLs, RPA (4.5 nM) and XPC-hHR23B (6.5 nM) were incubated, independently or together, for varying lengths of time with the radiolabeled Tdp-ICL substrate. As shown in Figure 4, the results indicate that RPA and XPC-hHR23B both interact with the damaged DNA substrate rapidly, with apparent half-maximal binding being achieved in less than four minutes for both XPC-hHR23B (Figure 4, lane 7) and RPA (Figure 4, lane 4). XPC-hHR23B bound ~25% of the available damaged substrate even at the <10 s time point (Figure 4, lane 5), compared to RPA which bound <5% (Figure 4, lane 1). These results suggest that XPC-hHR23B can bind to the Tdp-ICL substrate more rapidly than is detectable by this assay. As expected, based on the results shown in Figure 3, these concentrations of RPA (4.5 nM) and XPC-hHR23B (6.5 nM) resulted in only a minor formation of the higher-order product, as seen by the presence of a faint band migrating above damaged DNA substrate bound by XPC-hHR23B alone (Figure 4, lanes 9–12). Surprisingly, incubation of both proteins with the DNA substrate resulted in a slight increase in complex formation at the <10 s time-point, compared to the amount of substrate bound when incubated with the individual components (Figure 4, compare lane 9 to lanes 1 and 5). The mechanism of this interaction is not clear and further investigations using techniques with better time resolution are warranted.

XPC-hHR23B and XPA-RPA interact in the recognition of Tdp-ICLs

The higher-order complex seen in Figure 3 migrates in the gel at a position above that seen for either RPA or XPC-hHR23B when bound to the Tdp-ICL substrate. The presence of both XPC-hHR23B and RPA was confirmed by antibody super-shift assays using monoclonal antibodies directed against the 34 kDa subunit of RPA or to the maltose-binding protein tag present on the purified human recombinant XPC-hHR23B protein complex. Both the anti-RPA_{34} and anti-MBP antibodies were able to super-shift essentially 100% of the RPA-DNA or XPC-hHR23B-DNA complex (Figure 5, lanes 2 and 4, respectively). The presence of both XPC-hHR23B (at 6.5 nM) and RPA, at both low (4.5 nM; Figure 5, lanes 5–8) and high

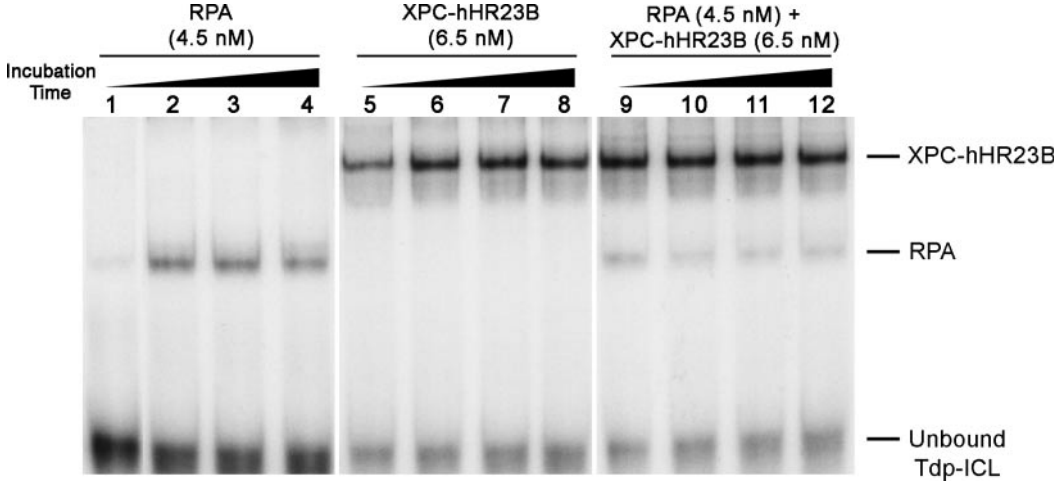

Figure 4. XPC-hHR23B demonstrates rapid binding to a Tdp-ICL substrate. RPA (4.5 nM, lanes 1–4), XPC-hHR23B (6.5 nM, lanes 5–8) or both proteins (Lanes 9–12) were incubated with the Tdp-ICL substrate (10 nM) and subjected to EMSA analysis. Incubation times were carried out for <10 s (lanes 1, 5 and 9), 1 (lanes 2, 6 and 10), 2 (lanes 3, 7 and 11) or 4 min (lanes 4, 8 and 12).

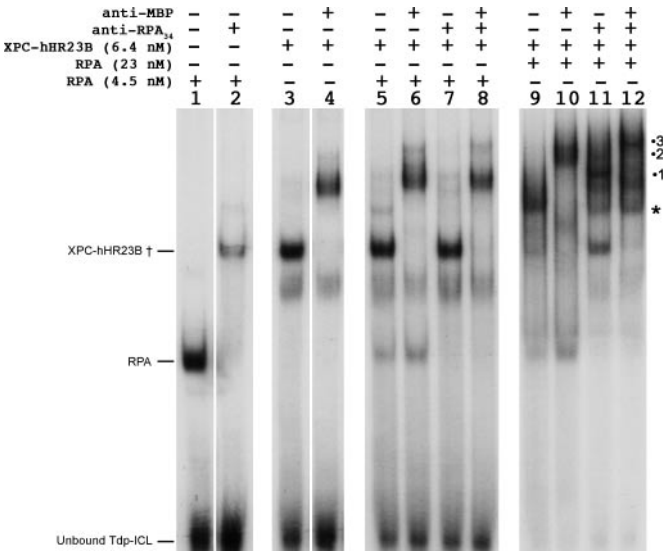

Figure 5. XPC-hHR23B and RPA are capable of simultaneously interacting with a Tdp-ICL substrate. All reactions were incubated with the Tdp-ICL substrate (10 nM) and protein, with or without monoclonal antibodies specific for the 34 kDa subunit of RPA or the MBP tag on the human recombinant XPC-hHR23B protein complex. All conditions were carried out as described in the experimental procedures. RPA: 4.5 nM (lanes 1, 2, 5–8) or 23 nM (lanes 9–12). XPC-hHR23B: 6.5 nM (lanes 3–12). Anti-RPA_{34}: 1 μg (lanes 2, 7, 8, 11, 12). Anti-MBP: 1 μg (lanes 4, 6, 8, 10, 12). †: RPA-Tdp-ICL super-shifted complex also migrated at the same position as when Tdp-ICL was bound by XPC-hHR23B. (*, •1, •2 and •3): see text for explanation.

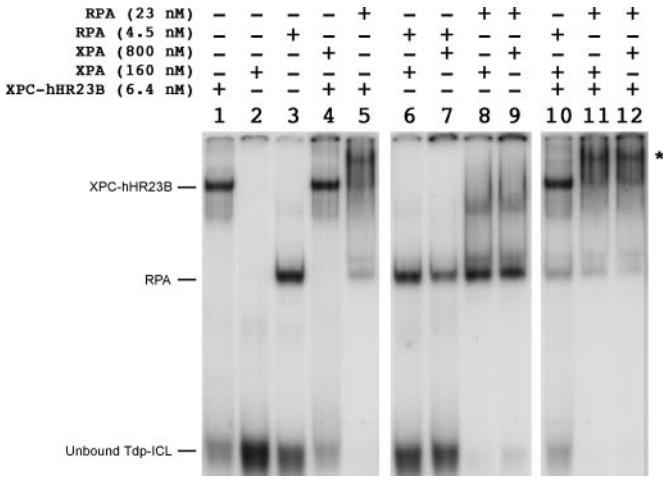

Figure 6. The XPA-RPA protein complex interacts with XPC-hHR23B on the Tdp-ICL in a similar fashion as RPA alone. All DNA–protein reactions were incubated and separated by EMSA as described in the experimental procedures. XPC-hHR23B was used at a single concentration of 6.5 nM (lanes 1, 4, 5, and 10–12). XPA was used at two different concentrations: 160 nM (lanes 2, 6, 8, 10 and 11) and 800 nM (lanes 3, 7, 9 and 12). RPA was also used at two concentrations of either 4.5 nM (lanes 3, 6, 7 and 10) or 23 nM (lanes 5, 8, 9, 11 and 12). *: ternary complex of XPC-hHR23B-XPA-RPA-Tdp-ICL.

(23.0 nM; Figure 5, lanes 9–12) concentrations, on the Tdp-ICL-protein shifted complex was confirmed by super-shifting by the antibodies. Formation of the higher-order complex (*) was observed in both instances (Figure 5) but represented the majority of the gel-shifted protein–DNA complexes when RPA was present at high concentrations (23 nM; Figure 5, lane 9). Addition of anti-MBP antibodies resulted in complete loss of the complex (*) and the appearance of a super-shifted product at both low (4.5 nM) and high (23.0 nM) concentrations of RPA (•2, Figure 5, lanes 6 and 10, respectively). In the presence of 4.5 nM or 23 nM RPA, anti-RPA_{34} also super-shifted the higher-order complex (*) to a position equivalent to the anti-MBP super-shifted XPC-hHR23B-Tdp-ICL complex (•1, Figure 5, lanes 7 and 11). Reappearance of the XPC-hHR23B-Tdp-ICL complex was observed when the anti-RPA_{34} antibody was added to the reaction in the presence of high concentrations of RPA (23 nM; Figure 5, lane 11), suggesting that the antibody may partially interfere with the formation of the higher-order complex. In the presence of 4.5 nM RPA and both antibodies (Figure 5, lane 8), a unique higher-order complex (•3) was observed to migrate slightly above the position of the super-shifted band in Figure 5 (lane 6). Using anti-RPA_{34} and anti-MBP with high concentrations of RPA in the reaction with XPC-hHR23B and the Tdp-ICL substrate resulted in a combination of banding patterns that were observed in the other lanes; however, the higher-order complex could be seen more intensely than the other bands (•3, Figure 5, lane 12). The antibodies were specific as neither demonstrated binding to the Tdp-ICL substrate alone nor the non-antigen protein (data not shown). The super-shifting of the higher-order complex by antibodies specific to either RPA or recombinant XPC-hHR23B supports our conclusion that both proteins may be able to cooperatively bind to the Tdp-ICL substrate, thereby forming a unique ternary complex.

We have previously shown, using antibody super-shift analyses, that XPA and RPA will form a ternary complex on a Tdp-ICL substrate (22). Here, formation of a higher-order complex was only seen in experiments that included high concentrations of RPA (≥9 nM) incubated with XPC-hHR23B. XPA alone did not exhibit similar behavior when incubated with XPC-hHR23B. To determine if there was interplay between XPC-hHR23B, XPA and RPA, these NER components were incubated in various combinations and concentrations with the Tdp-ICL substrate. XPC-hHR23B was present at 6.5 nM (Figure 6, Lanes 1, 4, 5 and 10–12), XPA was used either at 160 nM (Figure 6, lanes 2, 6, 8, 10 and 11) or 800 nM (Figure 6, lanes 4, 7, 9 and 12) and RPA was included at concentrations of either 4.5 nM (Figure 6, lanes 3, 6, 7 and 10) or 23 nM (Figure 6, lanes 5, 8, 9, 11 and 12). The results indicate that XPA (160 nM) alone did not shift the Tdp-ICL substrate (Figure 6, lane 2), or alter the mobility of an RPA-bound substrate at either 160 or 800 nM (Figure 6, compare lane 3 with lanes 6 and 7, respectively), as expected from our previously published results (22). Furthermore, the presence of XPA (160 or 800 nM) did not visibly alter the mobility of the higher-order complex (*, Figure 6, lanes 11 and 12), compared to reactions with XPC-hHR23B and RPA only (*, Figure 6, lane 6). These results demonstrate that the experimental outcome, when using the XPA-RPA complex and XPC-hHR23B, is indistinguishable from those experiments conducted with XPC-hHR23B and RPA only.

DISCUSSION

While unrepaired DNA damage threatens cell survival and proliferation, repair can introduce deleterious mutations.

The nature and frequency of these mutations are functions of the type of damage and the repair mechanisms that operate on them. DNA repair pathways are conveniently categorized according to the types of lesions with which they are associated, but there is growing evidence that there is considerable overlap and 'repair crosstalk' between these pathways [recently reviewed in (39)].

For example, both HR and NER participate in the removal of DNA ICLs in bacteria and yeast (10–12,40), however the mechanism of ICL repair in mammalian cells is not clear. Liu *et al*. (41) demonstrated that repair of mammalian DNA ICLs required members of the HR repair pathway since cells deficient in some of these proteins are highly susceptible to crosslinking compounds. Furthermore, it was recently shown that proteins from the mammalian mismatch repair (MMR) pathway may also play a role in the error-free removal of DNA ICLs (42,43). In addition, Wang *et al*. (44) demonstrated that constituents of the NER pathway facilitate the repair of ICLs in mammalian cells, but that the process occurred in a recombination-independent, error-generating fashion. Many different lines of evidence implicate the XPC-hHR23B protein complex as the primary initiating factor for DNA damage recognition in the GGR sub-pathway of NER [reviewed in (8) and references therein]. In a number of studies it has been demonstrated that the XPC-hHR23B protein complex is the first to bind damaged DNA and that XPA is not localized to DNA damage unless XPC-hHR23B is already present at the site of the lesion (24,45,46). The findings from those studies implicate XPC-hHR23B as a crucial component needed to initiate the repair of DNA damage that falls within the purview of the GGR pathway.

The XPA-RPA complex was previously observed to recognize psoralen-crosslinked triplex DNA substrates (22). In the work described here, we have presented the first biochemical evidence that XPC-hHR23B recognizes psoralen-crosslinked triplex DNA (Tdp-ICL) with high specificity and affinity (Figure 2). The recognition of the Tdp-ICL by XPC-hHR23B occurred within seconds of encountering the substrate, suggesting a very fast mechanism of recognition (Figure 4). A novel finding in the work presented here was that XPC-hHR23B (6.5 nM) and XPA (160 nM)-RPA (at concentrations $\geqslant$9 nM) were able to form a unique ternary complex (Figure 3) on the Tdp-ICL substrate, confirmed by antibody super-shift assay (Figure 5). Notably, incubation of both proteins with antibodies specific to either human recombinant XPC-hHR23B or RPA resulted in a complete loss of the higher-order complex (*, Figure 5) and the formation of a super-shifted complex with a lower mobility (•3, Figure 5, lanes 8 and 12) than was observed with incubation of the higher-order complex with either antibody alone. The observed antibody-antigen specificity strongly suggests that the uppermost super-shifted complex is indeed a complex of XPC-hHR23B-XPA-RPA on the damaged DNA substrate, representing a possible positive interaction between these proteins. These results implicate the GGR sub-pathway of NER as a possible mechanism for the removal of DNA ICLs in mammalian genomes. Although no direct protein–protein interaction has been demonstrated between XPC-hHR23B and RPA, it has been proposed that binding of XPC-hHR23B near a region of DNA damage induces a conformational change in the substrate and precipitates the formation of the NER pre-incision complex (24,47). Consistent with these findings, Reardon and Sancar (48,49) recently proposed that cooperation between NER pre-incision proteins (XPC-hHR23B, RPA and XPA) plus a kinetic proofreading function, supplied by TFIIH, could explain the ability of the NER pathway to detect and repair thymine dimers. They further hypothesized that increased specificity is accomplished through the interplay of proteins on neighboring or overlapping regions of DNA, independent of the order in which the proteins bind the damaged substrate, an idea that suggests a possible function for the higher order complexes we have observed in the work presented here.

Experiments using XPC-hHR23B and XPA (without RPA) demonstrated that XPA by itself was not enough to influence the recognition of the Tdp-ICL substrate by XPC-hHR23B (Figure 6, lane 4). The interaction of XPC-hHR23B with RPA (in the presence or absence of XPA) on ICL-containing substrates was also seen in experiments involving combinations of XPC-hHR23B, XPA and RPA at different concentrations (Figure 6). Interestingly, our results differ from those reported by You *et al*. (34) who showed that XPC-hHR23B physically interacted with XPA but that addition of both XPA and RPA displaced XPC-hHR23B from a substrate containing a *cis*-platin intrastrand crosslink. In our work, XPC-hHR23B and RPA competed for binding to the lesion at low concentrations of RPA but formed a complex on the damaged DNA including both XPC-hHR23B and XPA-RPA at high concentrations of RPA; the concentrations of RPA required are not inconsistent with a physiological role for this complex, given the high levels of RPA in the nucleus. It is possible that the types of complexes formed on the intrastrand crosslinks studied by You *et al*. (34) may differ from those formed on the ICLs studied here.

Wakasugi and Sancar (28) performed an experiment similar to ours using high concentrations of RPA (100 nM) with XPC (37 nM) on a single (6–4) photoproduct, but did not observe any evidence of a positive interaction between these proteins. Some possible reasons for this apparent discrepancy can be given. First, the lack of a higher-order complex could be due to their use of a substrate containing a different type of lesion, the (6–4) photoproduct. Second, they used XPC at a concentration that was <3-fold below that of RPA. In our experiments, formation of the ternary complex was most favorable when there was a 5-fold difference between the protein concentrations, although moderate formation of the higher-order complex could be seen with as low as a 3-fold difference in protein concentrations (*, Figure 3A and B, compare lanes 3 and 5).

There have been a number of studies that have confirmed the formation of an XPA-RPA-DNA complex (22,28,34, 50,51), but to our knowledge, no one has reported the formation of a ternary complex between ICL-damaged DNA, XPC-hHR23B, and RPA. The cellular concentrations of XPC, RPA and XPA have been estimated at $4–8 \times 10^4$ (52), 2.4×10^5 (53) and 5×10^4 (54) molecules per cell, respectively. We believe our experimental conditions reflect the presumed ratio of these NER factors in eukaryotic cells, thus supporting the possibility of an *in vivo* cooperative interaction between XPC-hHR23B and XPA-RPA in the recognition of psoralen-ICLs. The abundance of RPA suggests that it may play a role in determining the sensitivity of cells to DNA damage.

ACKNOWLEDGEMENTS

We thank Dr Theodore G. Wensel and Dr Rick A. Finch for advice and critical reading of the manuscript. We thank Sarah Henninger for her assistance in preparing this manuscript. This work is dedicated to the memory of Dr Peter Snow. This work was supported by a NCI Training Grant CA09480 (to BST) and NIH/NCI Grants CA93729 and CA97175 (to KMV). Funding to pay the Open Access publication charges for this article was provided by NIH/NCI Grant CA93729.

Conflict of interest statement. None declared.

REFERENCES

1. Mellon,I., Spivak,G. and Hanawalt,P.C. (1987) Selective removal of transcription-blocking DNA damage from the transcribed strand of the mammalian DHFR gene. *Cell*, **51**, 241–249.
2. Mellon,I. and Hanawalt,P.C. (1989) Induction of the *Escherichia coli* lactose operon selectively increases repair of its transcribed DNA strand. *Nature*, **342**, 95–98.
3. Wood,R.D. (1999) DNA damage recognition during nucleotide excision repair in mammalian cells. *Biochimie*, **81**, 39–44.
4. Iyer,N., Reagan,M.S., Wu,K.J., Canagarajah,B. and Friedberg,E.C. (1996) Interactions involving the human RNA polymerase II transcription/nucleotide excision repair complex TFIIH, the nucleotide excision repair protein XPG, and Cockayne syndrome group B (CSB) protein. *Biochemistry*, **35**, 2157–2167.
5. Selby,C.P. and Sancar,A. (1997) Human transcription-repair coupling factor CSB/ERCC6 is a DNA-stimulated ATPase but is not a helicase and does not disrupt the ternary transcription complex of stalled RNA polymerase II. *J. Biol. Chem.*, **272**, 1885–1890.
6. Tantin,D. (1998) RNA polymerase II elongation complexes containing the Cockayne syndrome group B protein interact with a molecular complex containing the transcription factor IIH components *Xeroderma pigmentosum* B and p62. *J. Biol. Chem.*, **273**, 27794–27799.
7. van Oosterwijk,M.F., Versteeg,A., Filon,R., van Zeeland,A.A. and Mullenders,L.H. (1996) The sensitivity of Cockayne's syndrome cells to DNA-damaging agents is not due to defective transcription-coupled repair of active genes. *Mol. Cell. Biol.*, **16**, 4436–4444.
8. Thoma,B.S. and Vasquez,K.M. (2003) Critical DNA damage recognition functions of XPC-hHR23B and XPA-RPA in nucleotide excision repair. *Mol. Carcinog.*, **38**, 1–13.
9. Dronkert,M.L. and Kanaar,R. (2001) Repair of DNA interstrand cross-links. *Mutat. Res.*, **486**, 217–247.
10. Van Houten,B., Gamper,H., Holbrook,S.R., Hearst,J.E. and Sancar,A. (1986) Action mechanism of ABC excision nuclease on a DNA substrate containing a psoralen crosslink at a defined position. *Proc. Natl Acad. Sci. USA*, **83**, 8077–8081.
11. Cole,R.S. (1973) Repair of DNA containing interstrand crosslinks in *Escherichia coli*: sequential excision and recombination. *Proc. Natl Acad. Sci. USA*, **70**, 1064–1068.
12. Jachymczyk,W.J., von Borstel,R.C., Mowat,M.R. and Hastings,P.J. (1981) Repair of interstrand cross-links in DNA of *Saccharomyces cerevisiae* requires two systems for DNA repair: the RAD3 system and the RAD51 system. *Mol. Gen. Genet.*, **182**, 196–205.
13. Joerges,C., Kuntze,I. and Herzinge,T. (2003) Induction of a caffeine-sensitive S-phase cell cycle checkpoint by psoralen plus ultraviolet A radiation. *Oncogene*, **22**, 6119–6128.
14. Guillonneau,F., Guieysse,A.L., Nocentini,S., Giovannangeli,C. and Praseuth,D. (2004) Psoralen interstrand cross-link repair is specifically altered by an adjacent triple-stranded structure. *Nucleic Acids Res.*, **32**, 1143–1153.
15. Perkins,B.D., Wensel,T.G., Vasquez,K.M. and Wilson,J.H. (1999) Psoralen photo-cross-linking by triplex-forming oligonucleotides at multiple sites in the human rhodopsin gene. *Biochemistry*, **38**, 12850–12859.
16. Vasquez,K.M., Wensel,T.G., Hogan,M.E. and Wilson,J.H. (1996) High-efficiency triple-helix-mediated photo-cross-linking at a targeted site within a selectable mammalian gene. *Biochemistry*, **35**, 10712–10719.
17. Vasquez,K.M. and Wilson,J.H. (1998) Triplex-directed modification of genes and gene activity. *Trends Biochem. Sci.*, **23**, 4–9.
18. Christensen,L.A., Conti,C.J., Fischer,S.M. and Vasquez,K.M. (2004) Mutation frequencies in murine keratinocytes as a function of carcinogenic status. *Mol. Carcinog.*, **40**, 122–133.
19. Vasquez,K.M., Narayanan,L. and Glazer,P.M. (2000) Specific mutations induced by triplex-forming oligonucleotides in mice. *Science*, **290**, 530–533.
20. Vasquez,K.M., Wang,G., Havre,P.A. and Glazer,P.M. (1999) Chromosomal mutations induced by triplex-forming oligonucleotides in mammalian cells. *Nucleic Acids Res.*, **27**, 1176–1181.
21. Vasquez,K.M., Marburger,K., Intody,Z. and Wilson,J.H. (2001) Manipulating the mammalian genome by homologous recombination. *Proc. Natl Acad. Sci. USA*, **98**, 8403–8410.
22. Vasquez,K.M., Christensen,J., Li,L., Finch,R.A. and Glazer,P.M. (2002) Human XPA and RPA DNA repair proteins participate in specific recognition of triplex-induced helical distortions. *Proc. Natl Acad. Sci. USA*, **99**, 5848–5853.
23. Evans,E., Moggs,J.G., Hwang,J.R., Egly,J.M. and Wood,R.D. (1997) Mechanism of open complex and dual incision formation by human nucleotide excision repair factors. *EMBO J.*, **16**, 6559–6573.
24. Sugasawa,K., Ng,J.M., Masutani,C., Iwai,S., van der Spek,P.J., Eker,A.P., Hanaoka,F., Bootsma,D. and Hoeijmakers,J.H. (1998) *Xeroderma pigmentosum* group C protein complex is the initiator of global genome nucleotide excision repair. *Mol. Cell*, **2**, 223–232.
25. Batty,D., Rapic'-Otrin,V., Levine,A.S. and Wood,R.D. (2000) Stable binding of human XPC complex to irradiated DNA confers strong discrimination for damaged sites. *J. Mol. Biol.*, **300**, 275–290.
26. Hey,T., Lipps,G., Sugasawa,K., Iwai,S., Hanaoka,F. and Krauss,G. (2002) The XPC-HR23B complex displays high affinity and specificity for damaged DNA in a true-equilibrium fluorescence assay. *Biochemistry*, **41**, 6583–6587.
27. Reardon,J.T. and Sancar,A. (2002) Molecular anatomy of the human excision nuclease assembled at sites of DNA damage. *Mol. Cell. Biol.*, **22**, 5938–5945.
28. Wakasugi,M. and Sancar,A. (1999) Order of assembly of human DNA repair excision nuclease. *J. Biol. Chem.*, **274**, 18759–18768.
29. Reardon,J.T., Mu,D. and Sancar,A. (1996) Overproduction, purification, and characterization of the XPC subunit of the human DNA repair excision nuclease. *J. Biol. Chem.*, **271**, 19451–19456.
30. Li,L., Peterson,C.A., Lu,X. and Legerski,R.J. (1995) Mutations in XPA that prevent association with ERCC1 are defective in nucleotide excision repair. *Mol. Cell. Biol.*, **15**, 1993–1998.
31. Christensen,J., Cotmore,S.F. and Tattersall,P. (1995) Minute virus of mice transcriptional activator protein NS1 binds directly to the transactivation region of the viral P38 promoter in a strictly ATP-dependent manner. *J. Virol.*, **69**, 5422–5430.
32. Sugasawa,K., Okamoto,T., Shimizu,Y., Masutani,C., Iwai,S. and Hanaoka,F. (2001) A multistep damage recognition mechanism for global genomic nucleotide excision repair. *Genes Dev.*, **15**, 507–521.
33. Kusumoto,R., Masutani,C., Sugasawa,K., Iwai,S., Araki,M., Uchida,A., Mizukoshi,T. and Hanaoka,F. (2001) Diversity of the damage recognition step in the global genomic nucleotide excision repair *in vitro*. *Mutat. Res.*, **485**, 219–227.
34. You,J.S., Wang,M. and Lee,S.H. (2003) Biochemical analysis of the damage recognition process in nucleotide excision repair. *J. Biol. Chem.*, **278**, 7476–7485.
35. Yokoi,M., Masutani,C., Maekawa,T., Sugasawa,K., Ohkuma,Y. and Hanaoka,F. (2000) The *Xeroderma pigmentosum* group C protein complex XPC-HR23B plays an important role in the recruitment of transcription factor IIH to damaged DNA. *J. Biol. Chem.*, **275**, 9870–9875.
36. Svejstrup,J.Q., Wang,Z., Feaver,W.J., Wu,X., Bushnell,D.A., Donahue,T.F., Friedberg,E.C. and Kornberg,R.D. (1995) Different forms of TFIIH for transcription and DNA repair: holo-TFIIH and a nucleotide excision repairosome. *Cell*, **80**, 21–28.
37. Maldonado,E., Shiekhattar,R., Sheldon,M., Cho,H., Drapkin,R., Rickert,P., Lees,E., Anderson,C.W., Linn,S. and Reinberg,D. (1996) A human RNA polymerase II complex associated with SRB and DNA-repair proteins. *Nature*, **381**, 86–89.
38. Drapkin,R., Reardon,J.T., Ansari,A., Huang,J.C., Zawel,L., Ahn,K., Sancar,A. and Reinberg,D. (1994) Dual role of TFIIH in DNA excision repair and in transcription by RNA polymerase II. *Nature*, **368**, 769–772.

39. Sancar,A., Lindsey-Boltz,L.A., Unsal-Kaccmaz,K. and Linn,S. (2004) Molecular mechanisms of mammalian DNA repair and the DNA damage checkpoints. *Annu. Rev. Biochem.*, **73**, 39–85.
40. Cole,R.S., Levitan,D. and Sinden,R.R. (1976) Removal of psoralen interstrand cross-links from DNA of *Escherichia coli*: mechanism and genetic control. *J. Mol. Biol.*, **103**, 39–59.
41. Liu,N., Lamerdin,J.E., Tebbs,R.S., Schild,D., Tucker,J.D., Shen,M.R., Brookman,K.W., Siciliano,M.J., Walter,C.A., Fan,W. *et al.* (1998) XRCC2 and XRCC3, new human Rad51-family members, promote chromosome stability and protect against DNA cross-links and other damages. *Mol. Cell*, **1**, 783–793.
42. Zhang,N., Lu,X., Zhang,X., Peterson,C.A. and Legerski,R.J. (2002) hMutSbeta is required for the recognition and uncoupling of psoralen interstrand cross-links *in vitro*. *Mol. Cell. Biol.*, **22**, 2388–2397.
43. Wu,Q., Christensen,L.A., Legerski,R.J. and Vasquez,K.M. (2005) Mismatch repair participates in an error-free processing of DNA interstrand crosslinks in human cells. *EMBO Reports*, in press.
44. Wang,X., Peterson,C.A., Zheng,H., Nairn,R.S., Legerski,R.J. and Li,L. (2001) Involvement of nucleotide excision repair in a recombination-independent and error-prone pathway of DNA interstrand cross-link repair. *Mol. Cell. Biol.*, **21**, 713–720.
45. Volker,M., Mone,M.J., Karmakar,P., van Hoffen,A., Schul,W., Vermeulen,W., Hoeijmakers,J.H., van Driel,R., van Zeeland,A.A. and Mullenders,L.H. (2001) Sequential assembly of the nucleotide excision repair factors *in vivo*. *Mol. Cell*, **8**, 213–224.
46. Riedl,T., Hanaoka,F. and Egly,J.M. (2003) The comings and goings of nucleotide excision repair factors on damaged DNA. *EMBO J.*, **22**, 5293–5303.
47. Sugasawa,K., Shimizu,Y., Iwai,S. and Hanaoka,F. (2002) A molecular mechanism for DNA damage recognition by the *Xeroderma pigmentosum* group C protein complex. *DNA Repair (Amst.)*, **1**, 95–107.
48. Reardon,J.T. and Sancar,A. (2004) Thermodynamic cooperativity and kinetic proofreading in DNA damage recognition and repair. *Cell Cycle*, **3**, 141–144.
49. Reardon,J.T. and Sancar,A. (2003) Recognition and repair of the cyclobutane thymine dimer, a major cause of skin cancers, by the human excision nuclease. *Genes Dev.*, **17**, 2539–2551.
50. Buschta-Hedayat,N., Buterin,T., Hess,M.T., Missura,M. and Naegeli,H. (1999) Recognition of nonhybridizing base pairs during nucleotide excision repair of DNA. *Proc. Natl Acad. Sci. USA*, **96**, 6090–6095.
51. Missura,M., Buterin,T., Hindges,R., Hubscher,U., Kasparkova,J., Brabec,V. and Naegeli,H. (2001) Double-check probing of DNA bending and unwinding by XPA-RPA: an architectural function in DNA repair. *EMBO J.*, **20**, 3554–3564.
52. van der Spek,P.J., Eker,A., Rademakers,S., Visser,C., Sugasawa,K., Masutani,C., Hanaoka,F., Bootsma,D. and Hoeijmakers,J.H. (1996) XPC and human homologs of RAD23: intracellular localization and relationship to other nucleotide excision repair complexes. *Nucleic Acids Res.*, **24**, 2551–2559.
53. Seroussi,E. and Lavi,S. (1993) Replication protein A is the major single-stranded DNA binding protein detected in mammalian cell extracts by gel retardation assays and UV cross-linking of long and short single-stranded DNA molecules. *J. Biol. Chem.*, **268**, 7147–7154.
54. Cleaver,J.E. and Kraemer,K.H. (1995) *Xeroderma pigmentosum* and Cockayne syndrome. In Scriver,C. R. (ed.), *The Metabolic and Molecular Bases of Inherited Disease*, 7th edn. McGraw-Hill Health Professions Division, NY, Vol. 3, pp. 3 v. (xxxvi, 4605, 4693).